

# Degree of substitution of chlorin $e_6$ on charged poly- L-lysine chains affects their cellular uptake, localization and phototoxicity towards macrophages and cancer cells

Michael R. Hamblin<sup>a,b,\*</sup>, Jaimie L. Miller<sup>a</sup>, Imran Rizvi<sup>a</sup> and Bernhard Ortel<sup>a,b</sup>

<sup>a</sup>*Wellman Laboratories of Photomedicine, WEL224, Massachusetts General Hospital, Boston, MA 02114, USA*

<sup>b</sup>*Department of Dermatology, Harvard Medical School, MA. 02115, USA*

**Abstract.** Macromolecular photosensitizer conjugates are under investigation as improved delivery vehicles for dyes used in photodynamic therapy. We have previously described the use of conjugates between photosensitizers such as chlorin<sub>*e*6</sub> ( $C_{e6}$ ) and poly-L-lysine (pL) chains which are versatile molecular species because the size of the chain can be varied, and the overall charge can be altered from cationic through neutral to anionic. We now report on a series of pL- $C_{e6}$  conjugates in their cationic (native), neutral (acetylated) and anionic (succinylated) forms, where the number of  $C_{e6}$  molecules attached to each chain was varied (pL:  $C_{e6}$  ratios, 1:4, 1:8, 1:12, and 1:16). The fluorescence emissions were measured in both saline and a disaggregating solvent. We studied two cell lines (an epithelial ovarian cancer, OVCAR-5 and a mouse macrophage, J774) and measured cellular uptake, subcellular localization (by confocal fluorescence microscopy) and phototoxicity. The cellular uptake of the conjugates with four substitution ratios all delivered at 2  $\mu$ M  $C_{e6}$  equivalent concentration showed a maximum at 12  $C_{e6}$  per chain for both cationic and anionic conjugates, but the uptake of the neutral conjugate was proportional to the substitution ratio. The macrophages took up several times more  $C_{e6}$  than the ovarian cancer cells. Confocal fluorescence micrographs showed more cellular fluorescence with the lower substitution ratios, and more lysosomal localization with the cationic conjugates. The phototoxicity was much higher for the neutral conjugates. For the cationic and neutral conjugates the 12  $C_{e6}$  per chain was the most effective at killing cells, while for the anionic conjugate it was the 16  $C_{e6}$  per chain. The anionic conjugate was better at killing OVCAR-5 cells, while the cationic was better for J774 cells, and the neutral was approximately the same. These data will help to optimize the parameters to be used in preparing polymeric-photosensitizer conjugates for photodynamic therapy.

Keywords: Photodynamic therapy, photosensitizer, polymeric drug conjugate, confocal fluorescence microscopy, macrophage, cancer

## 1. Introduction

The selective accumulation and/or retention of a photosensitizer (PS) in neoplastic tissues is essential for the efficacy of photodynamic therapy (PDT) of tumors. It is determined, among other factors, by

---

\*Corresponding author and Author to whom proofs and reprint requests should be addressed. Fax: +1 617 726 8566; E-mail: hamblin@helix.mgh.harvard.edu.

the hydrophobicity and aggregated state of the PS, decreased pH in tumors, tumor neovascular effects, poorly developed tumor lymphatics, and differences in the stromal cells (particularly macrophages) within the tumor [1]. Because most PS used in PDT have limited selectivity for tumor tissue [2] several groups have aimed to increase the specificity of PS for tumors by conjugate and complex formation with macromolecular carriers [3]. One method of targeting drugs, radioisotopes and recently PS to tumors which is attracting interest, is the use of polymer-conjugates. These may be either natural polymers such as dextran [4] and polyamino-acids [5], or synthetic polymers such as N-(2-hydroxypropyl)methacrylamide [6]. There have been reports of PS being conjugated to polymeric carries [7,8], but these have not focused on the role of the charge borne by the conjugate.

We originally designed poly-L-lysine chlorin( $c_{e6}$ ) (pL- $c_{e6}$ ) conjugates as vehicles to attach a number of PS molecules to monoclonal antibodies in a site-specific manner for photoimmunotherapy (antibody-mediated PS delivery) [9]. Because the construct consisting of an antibody bound to a pL chain with a relatively small number of  $c_{e6}$  molecules attached to the epsilon amino groups had a pronounced cationic charge, we investigated the possibility of rendering the molecule anionic by treating the remaining epsilon amino groups with succinic anhydride [10–12]. We subsequently studied the use of the pL- $c_{e6}$  conjugates themselves as PS delivery vehicles and compared the cationic and anionic species with a neutral molecule obtained by treating the epsilon amino groups with acetic anhydride [13]. Cationic and anionic conjugates formed from two sizes of pL chains were studied in a rat orthotopic cancer model [14], and the effect of attaching polyethylene glycol (PEG) side chains to the acet pL- $c_{e6}$  conjugates was investigated both in vitro and in a mouse model of metastatic ovarian cancer [15]. Recently we have reported that the cationic pL- $c_{e6}$  species are highly effective for as delivery vehicles for PDT of bacteria both in vitro [16, 17] and in mouse models of wound infections [18].

In addition to the above-mentioned important variables in the molecular design (size of the pL chain and overall charge), another variable that should be considered is the substitution ratio (SR), i.e., the number of molecules of  $c_{e6}$  attached to each chain. This is expected to be important because of the well-known tendency of tetrapyrrole molecules to undergo self-association both in intermolecular and intramolecular fashions. If the  $c_{e6}$  molecules are bound close together on the pL chains, this might be expected to affect their photophysical properties such as fluorescence and triplet yields, and the changes to the overall molecular structure may impact their interaction with cells such as uptake, subcellular localization and consequent phototoxicity. We now report on a series of pL- $c_{e6}$  conjugates prepared with four SRs (pL: $c_{e6}$ , 1:4, 1:8, 1:12, and 1:16) and subsequently either left cationic or rendered neutral or anionic as described above. The fluorescence emissions were measured both in saline and a disaggregating solvent. We studied two cell lines (an epithelial ovarian cancer, OVCAR-5 and a mouse macrophage, J774) and measured cellular uptake, subcellular localization (by confocal fluorescence microscopy) and phototoxicity.

## 2. Materials and methods

### 2.1. Preparation of polylysine $c_{e6}$ conjugates of varying charges

The N-hydroxysuccinimide ester of  $c_{e6}$  (Porphyrin Products, Logan, UT) was prepared by reacting 1.5 equivalents of dicyclohexylcarbodiimide and 1.5 equivalents of N-hydroxysuccinimide with 1 equivalent of  $c_{e6}$  in dry dimethyl sulfoxide (DMSO). Four portions each of 40 mg (2.1  $\mu$ mol) poly-L-lysine hydrobromide (Sigma, St Louis, MO) (average M.Wt. 18,600, average degree of polymerization = 89) were dissolved in dry DMSO (20 mL) containing N-ethylmorpholine (1 mL). To these four solutions were

added 0.2 mL, 0.4 mL, 0.8 mL and 1.6 mL of a dry DMSO solution containing  $c_{e6}$ -N-hydroxysuccinimide ester (25 mg/mL, containing 8.3, 16.7, 25 and 33.3  $\mu\text{mol}$  of  $c_{e6}$  respectively) and the solutions were kept in the dark at room temperature for 24 h. Each solution was then divided into three equal portions. One set of four preparations of the different SRs was saved unmodified, while a second set of four was treated with an excess of acetic anhydride (100 mg dissolved in 0.5 mL dry DMSO) to produce a set of neutral charged conjugates, and the third set of four was treated with an excess of succinic anhydride (100 mg dissolved in 0.5 mL dry DMSO) to produce an anionic charge. These twelve solutions were dialyzed in DMSO-resistant dialysis membrane of 3500 MW cutoff (Spectrum Medical Industries, Los Angeles, CA) for 24 h against three changes of 10 mM phosphate buffer (pH = 7). All experimental manipulations of preparations containing  $c_{e6}$  were carried out in subdued lighting.

## 2.2. Absorbance and fluorescence spectroscopy

The degree of  $c_{e6}$  substitution on the polylysine chains was estimated by measuring the absorbance at 400 nm of conjugates dissolved in 0.1 M NaOH/0.1% SDS and calculating the amount of  $c_{e6}$  present using  $\epsilon_{400\text{ nm}} = 150000$ . The amount of pL was assumed to be the original quantity weighed out. After exhaustive dialysis it was assumed that the remaining  $c_{e6}$  was covalently bound to the pL. The fluorescence emission spectra of the pL- $c_{e6}$  conjugates in 0.1 M NaOH and also in PBS were measured as a function of the  $c_{e6}$  absorbance at 400 nm and were recorded from 580–720 nm after excitation at 400 nm using quartz cuvetts with 1 cm path length on a spectrofluorimeter (Fluorolog 3, SPEX Industries, Edison, NJ).

## 2.3. Cells and culture conditions.

NIH:OVCAR-5 (OVCAR-5) cells were obtained from Dr. T. Hamilton (Fox Chase Cancer Institute, Philadelphia, PA) and J774.A1 (J774) mouse macrophage-like cells were from ATCC (Rockville, MD). Cells were grown in RPMI-1640 media containing Hepes, glutamine, 10% heat-inactivated fetal calf serum (FCS), 100 U/mL penicillin and 100  $\mu\text{g/mL}$  streptomycin at 37°C in a humidified 5%  $\text{CO}_2$  atmosphere.

## 2.4. Cellular uptake

Cells were seeded into 24-well plates, allowed to resume exponential growth (70% confluent), at which time medium was removed and replaced with growth medium with 10% FCS containing 2- $\mu\text{M}$   $c_{e6}$  equivalent (final concentration in medium) in triplicate. After 6 h the conjugate solution was aspirated from the wells, the cells were washed with PBS and incubated with 1mL trypsin-EDTA (Gibco, Invitrogen Corp, Carlsbad, CA) for 10 min. The resulting cell suspension was then centrifuged, the trypsin supernatant was aspirated and retained and the pellets (visibly fluorescent under long wave UV) were dissolved in 1.5 mL 0.1 M NaOH/1% SDS for at least 24 h to give a homogenous solution. The fluorescence of the cell extract was measured on a spectrofluorimeter as described above. The protein content of the entire cell extract was then determined by a modified Lowry method [19] using bovine serum albumin dissolved in 0.1M NaOH/1% SDS to construct calibration curves. The trypsin supernatant checked for the presence of fluorescence which was negligible. Results were expressed as mol of  $c_{e6}$  per mg cell protein determined from fluorescence intensity calibration curves prepared separately for all 12 conjugates.

### 2.5. Confocal microscopy.

Cells ( $2 \times 10^5$ ) were plated on a  $20 \times 20$  mm microscope cover slip and incubated for at least 24 hours. The conjugates were dissolved in complete medium at a concentration of  $2\text{-}\mu\text{M}$   $c_{e6}$  equivalent, added to the cells and incubated for 6 h. The cells were rinsed and mounted with PBS on a microscope slide using 0.02-mm thick distance holders in order to prevent compression of the cells. A confocal laser microscope (Leica Mikroskopie und System GmbH, Wetzlar, Germany) consisting of a Leica TCS 4D scanner attached to a Leitz DM IRD microscope was operated using the TCS-NT software package (Leica Lasertechnik, Heidelberg, Germany). An argon laser at 488-nm was used for excitation. A  $40 \times$  air or  $100 \times$  oil immersion objective was used to image at a  $1024 \times 1024$  pixels resolution. Two channels collected fluorescence signals in either the green range (580 nm dichroic mirror plus 530-nm bandpass filter) or the red range (580 nm dichroic mirror plus 590-nm longpass filter). The green and red ie color output) were superimposed for the figures.

### 2.6. Phototoxicity

This was carried out essentially as previously described [13]. Briefly, cells were cultured in 96-well plates for 24 h until 70% confluent. Conjugates were added in complete medium at a final concentration of  $2\text{-}\mu\text{M}$   $c_{e6}$  equivalent and incubated for 6 h. Cells were washed twice and fresh medium was added. An argon pumped dye laser (Innova 100: CR-599 Coherent, Inc., Palo Alto, CA) was tuned to 666 nm and coupled into a 1 mm quartz fiber and objective lens to create a homogeneous spot which delivered light from below to the wells with fluences delivered ranging from 0 to  $10 \text{ J/cm}^2$  at a fluence rate of  $50 \text{ mW/cm}^2$ . After illumination cells were incubated with fresh medium for 24 h. Controls were: light alone, conjugate and kept out of the incubator in the dark for the duration of the illumination, neither light nor conjugate. Survival fraction was quantified with the MTT assay [20] and read in an automatic microplate reader at 560 nm. Survival fraction was calculated as the mean formance from PDT treated cells divided by the mean absorbances from dark controls incubated with conjugate.

## 3. Results

### 3.1. Conjugates

Figure 1 shows the synthetic scheme for the conjugates. The four substitution ratios (referred to as 4, 8, 12, and 16 SR) were calculated to be  $3.85 \pm 0.7$ ,  $7.9 \pm 0.4$ ,  $12.29 \pm 0.8$ , and  $16.23 \pm 0.9$   $c_{e6}$  per chain of 89 lysine residues respectively. Since there were three independent determinations of each SR derived from measurements of the cationic, neutral and anionic conjugates, the numbers given are the mean  $\pm$  SD of 3 measurements.

### 3.2. Fluorescence

Figures 2a, b, and c show the relationship between the fluorescence emission and the absorbance at 400 nm for the conjugates dissolved in both 0.1 M NaOH and also in PBS. For the cationic conjugates Fig. 2a shows that the four SRs have similar fluorescence yields when dissolved in NaOH, but in PBS the overall fluorescence was dramatically lower (from one quarter to one twenty-fifth of the magnitude measured in NaOH), and in addition the fluorescence of the individual conjugates was proportional to the

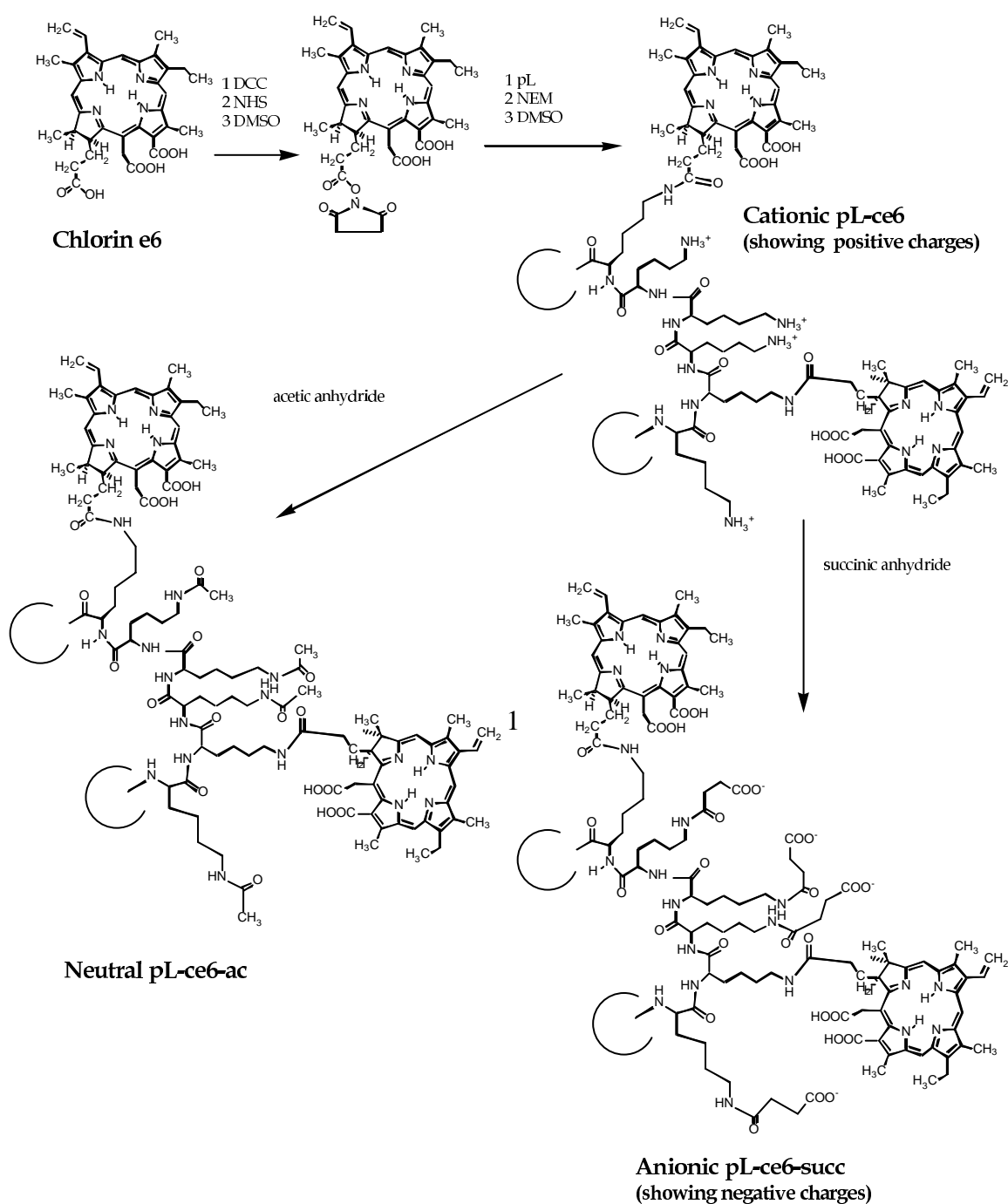


Fig. 1. Synthetic scheme for the preparation of cationic, neutral and anionic conjugates.

SR with the 16 SR conjugate having about 7 times as much fluorescence as the 4 SR conjugate. Figure 2b shows the corresponding relationship for the neutral conjugates. Here, as before, all 4 conjugates had similar fluorescence yields when dissolved in NaOH, but in PBS the reduction in fluorescence was not

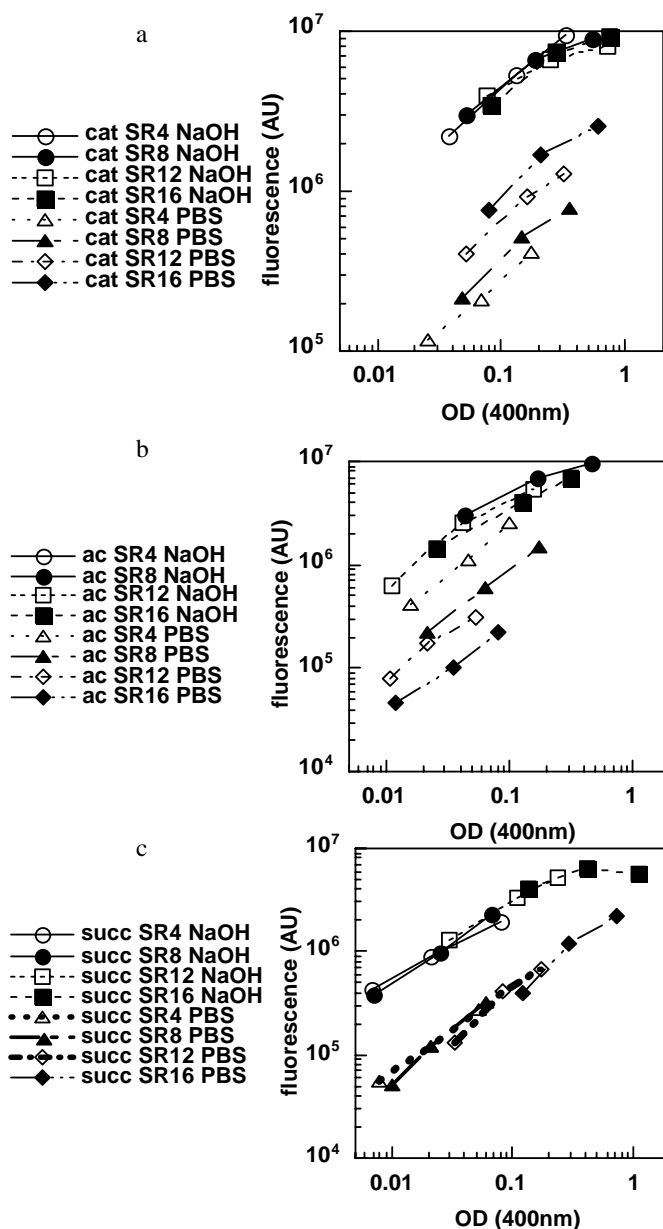


Fig. 2. Relationship between the fluorescence emission intensity at 668 nm and the absorbance at 400 nm measured in either 0.1 M NaOH or PBS for 4 SR conjugates with varying charges, a) cationic pL-Ce6; b) neutral pL-Ce6-ac; c) anionic pL-Ce6-succ.

as pronounced (from 8–50% of the values found in NaOH). The relationship between the fluorescence and SR was opposite to that found with the cationic conjugates, being inversely proportional to the SR, with the 4 SR conjugate having almost 10 times as much fluorescence as the 16 SR conjugate. Figure 2c shows the same experiment performed for the 4 anionic conjugates. Here there is yet another pattern displayed, with all four SR conjugates having similar fluorescence yields, and the values in NaOH being approximately 10 times bigger than those in PBS.

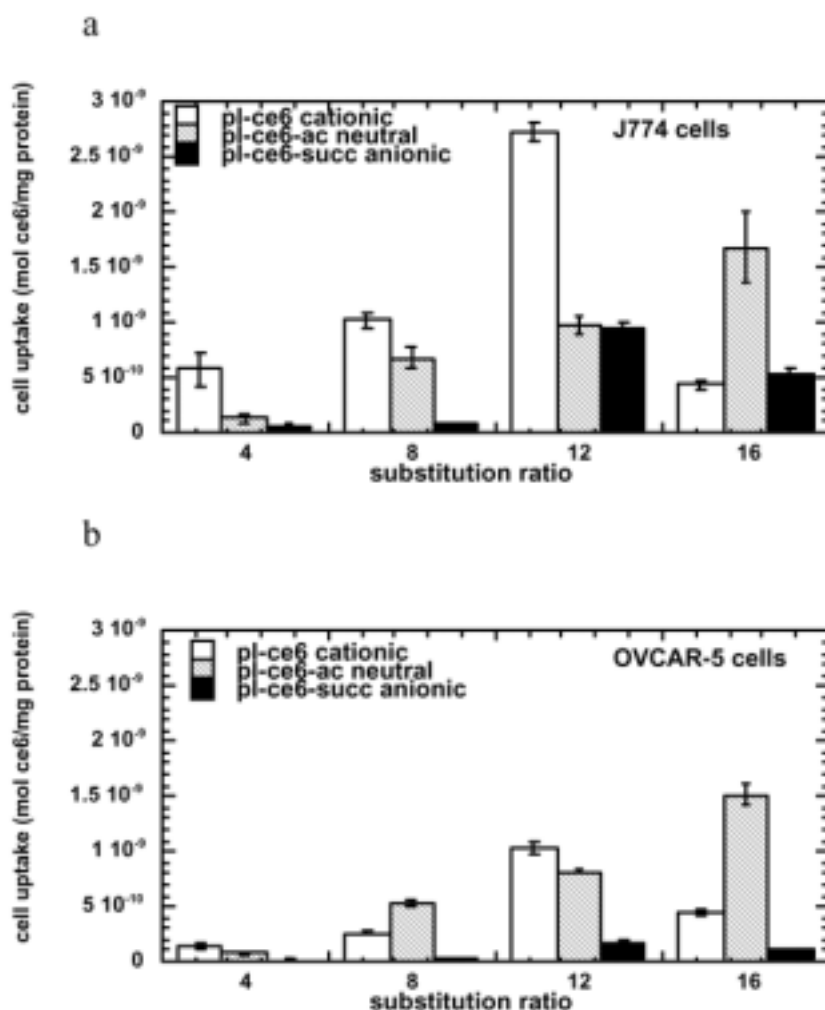


Fig. 3. Uptake of the 12 conjugates all delivered to the cells at a concentration of  $2 \mu\text{M}$   $c_{e6}$  equivalent and incubated for 6 h in complete medium by a) J774 mouse macrophages and b) OVCAR-5 cancer cells. Values are means of three separate experiments and bars are SEM.

### 3.3. Uptake

Figure 3a shows the uptakes of the 12 conjugates representing the four SRs and three charges by J774 mouse macrophages. For the SRs of 4 and 8  $c_{e6}$  per chain the order of uptake was cationic > neutral > anionic. At 12 SR the uptake of the cationic conjugate was highest whilst that of the neutral and anionic conjugates was similar. At 16 SR the neutral conjugate had a higher uptake than both the cationic and anionic conjugates. The overall result was that both the cationic and anionic conjugates showed maximum uptakes at a SR of 12, while the uptake of the neutral conjugate increased with increasing SR.

Figure 3b shows the equivalent cellular uptake of the 12 conjugates by OVCAR-5 ovarian cancer cells. The general pattern of variation in uptakes is similar to that seen in J774 cells, except that the uptakes are mostly substantially smaller (down to 15% of the uptake seen with J774 cells). In Table 1 we show the ratio of the uptakes between J774 and OVCAR-5 cells. The cationic conjugates show a trend for a

Table 1  
Ratio of cellular uptakes of  $c_{e6}$  between J774 cells and OVCAR-5 cells. Numbers were derived from data in Figs 3a and 3b

SR	cationic	neutral	anionic
4	4.2	1.6	4.0
8	3.9	1.3	4.2
12	2.7	1.2	5.2
16	1.0	1.1	5.3

comparatively higher uptake by J774 cells to decrease with increasing SR until the uptake is equal for both cell lines with the 16 SR. The neutral conjugates show a similar but less pronounced reduction in preferential uptake by macrophages with increasing SR. By contrast the anionic series all have a higher uptake by macrophages, which increases even further with increasing SR.

### 3.4. Confocal fluorescence microscopy

Figure 4 illustrates the fluorescence emissions of  $c_{e6}$  taken up from the conjugates into J774 and OVCAR-5 cells. The red  $c_{e6}$  fluorescence is superimposed on the green autofluorescence which is emitted from intracellular organelles including mitochondria and lysosomes. Although it is not generally possible to use the intensity of fluorescence from confocal micrographs as a quantitative measure to compare levels of uptake, the large variations in fluorescence intensity observed in these images deserve mention. The cationic conjugates give punctate intracellular red fluorescence that becomes more confined with increasing SR. The fluorescence from the neutral conjugates in both cell lines decreases as the SR increases, while the fluorescence from the anionic conjugates increases with increasing SR in both cell lines.

## 4. Phototoxicity

The survival fractions as determined by the MTT assay for mitochondrial dehydrogenase activity were measured as a function of increasing fluences of 666 nm light delivered. Figures 5a and 5b show the phototoxicity of the cationic conjugates against J774 and OVCAR-5 cells. In both cases the 12 SR gave the highest phototoxicity, while for the OVAR-5 cells the 16 SR was second in effectiveness, and for J774 cells it was the 8 SR. There was significantly more killing observed for all SRs against J774 cells compared to that found for OVCAR-5 cells.

Figures 5c and 5d show the phototoxicity curves for J774 and OVCAR-5 cell lines using the 4 SRs and neutral conjugates. There was much more killing of both cell lines compared to the 4 cationic conjugates. In both cell lines the 12 SR conjugate was by far the most effective, leading to >99% toxicity after 10 J/cm<sup>2</sup> light, followed by the conjugate with 8 SR. There did not appear to be any major differences between the amounts of killing observed with OVCAR-5 and J774 cells.

Figures 5e and 5f show the corresponding killing curves for the 4 SRs and anionic conjugates. In the case of OVCAR-5 cells the order of the effectiveness in killing is the increasing SR, with the 16 SR conjugate producing 85% toxicity at 10 J/cm<sup>2</sup>. With J774 cells the 4 and 8 SR conjugates produced an increase in MTT activity compared to dark controls at light doses of 2 and 5 J/cm<sup>2</sup> compared to dark controls, but this effect disappeared at 10 J/cm<sup>2</sup>. The 12 and 16 SR conjugates produced killing at all fluences, but the SR 16 particularly gave more killing of OVCAR-5 cells compared to J774.



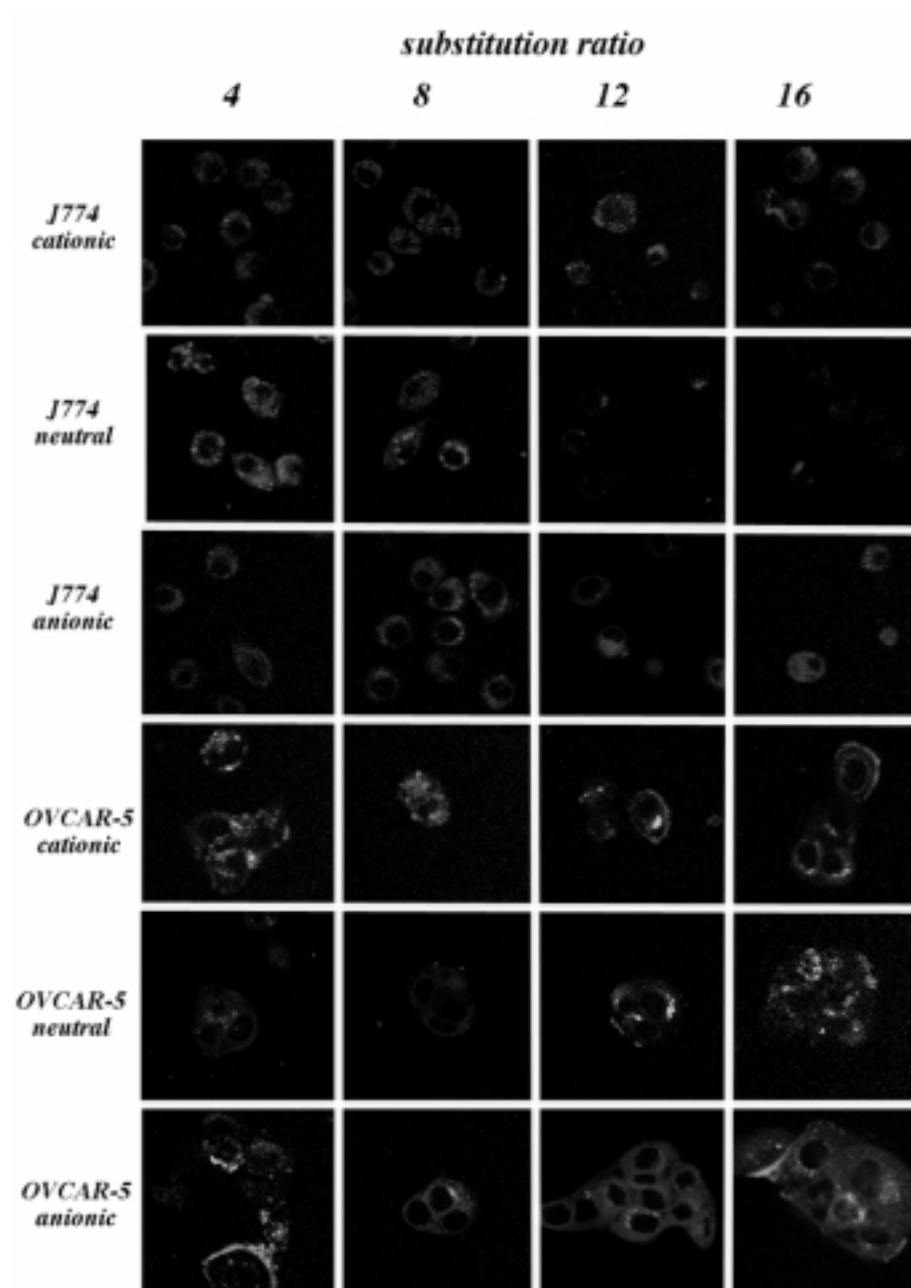


Fig. 4. Confocal fluorescence micrographs of J774 cells (upper rows) and OVCAR-5 cells (lower rows) incubated for 6 h with  $2 \mu\text{M}$   $c_{e6}$  equivalent of 4 SRs (columns) of conjugates of different charges. Red  $c_{e6}$  fluorescence is superimposed on green autofluorescence. Bar =  $10 \mu\text{m}$ .

## 5. Discussion

Polymer-PS conjugates may be useful agents for delivering PS to cells in vitro and to tumors and other pathological lesions in vivo, and pL is likely to be the polymeric scaffold of choice due to its inherent

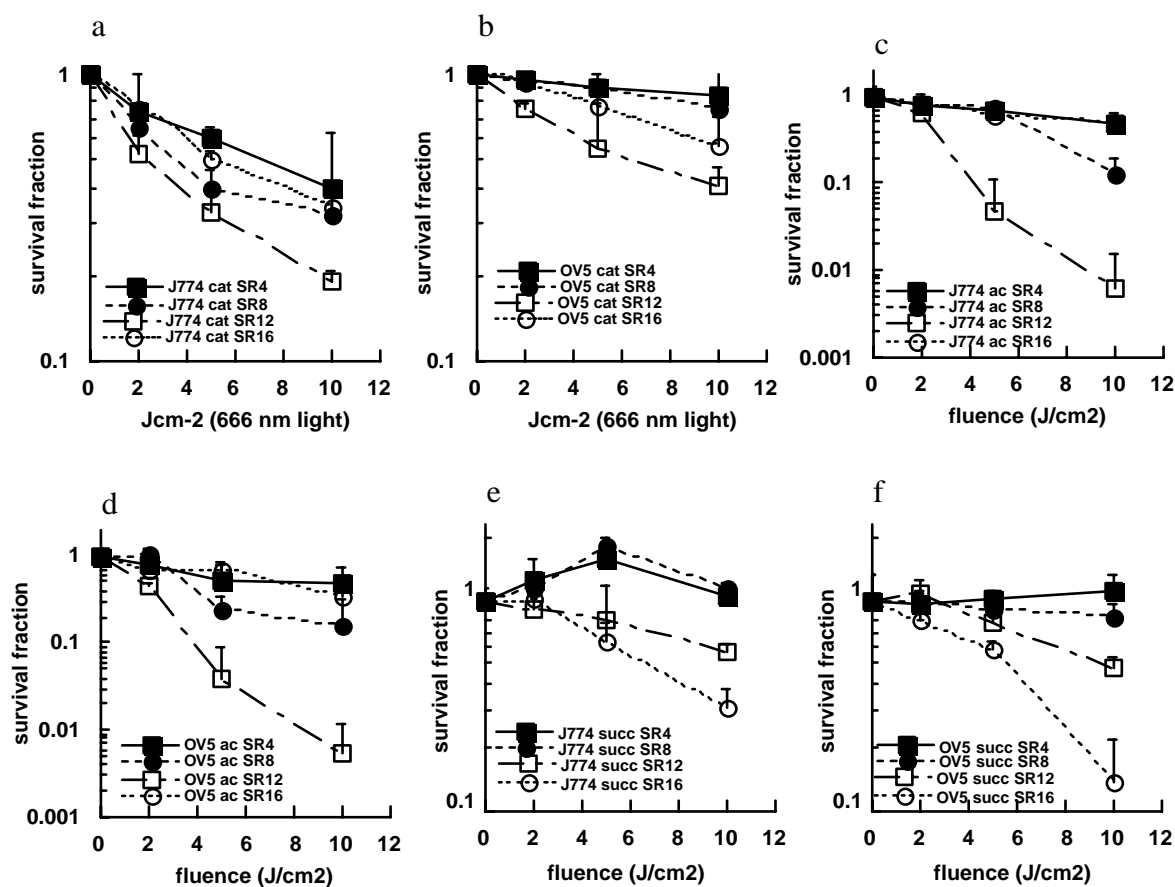


Fig. 5. Survival curves for PDT of cells loaded with the conjugates delivered at  $2 \mu\text{M}$   $c_{e6}$  equivalent concentration, incubated for 6 h and exposed to increasing fluences of 666 nm light in complete medium. MTT activity was measured 24 hours later. Points are means of 3 independent experiments and bars are SEM. a) J774 cells and cationic conjugates, b) OVCAR-5 cells and cationic conjugates, c) J774 cells and neutral conjugates, d) OVCAR-5 cells and neutral conjugates, e) J774 cells and anionic conjugates, f) OVCAR-5 cells and anionic conjugates.

versatility. This versatility lies in the ability to rationally vary parameters such as the size of the pL chain, the overall charge and hydrophobicity by attaching side chains such as acetyl, succinyl or PEG, and the density of PS molecules attached along the chain. The present study has investigated the effect of varying the number of  $c_{e6}$  molecules attached to each pL chain. Because of the synthesis strategy whereby the acetyl or succinyl groups are attached after the  $c_{e6}$  molecules, the SRs are directly comparable between chains of varying charges. We studied two cell lines, ovarian cancer cells and a mouse macrophage cell line. It has been shown that PDT of tumors can proceed by three distinct mechanisms [21], a) direct killing of tumor cells that hashutdown of the tumor vasculature after PDT mediated thrombosis and vascular damage, and c) activation of the host immune system leading to a long lasting anti-tumor response. Tumor-associated macrophages have been reported to accumulate large amounts of PS in vivo [22] and this is also likely to apply to macromolecular-PS conjugates. The preservation of macrophage function in tumors after PDT may be desirable to encourage the acute inflammatory response and the long-term anti-tumor immune response [23]; both of which have been proposed to be important in the therapeutic outcome [24].

The structure of the conjugates in the present study inherently involves the possibility of molecular interaction of the tetrapyrrole moieties that are attached along the pL chain. As the SR is increased the chances of this interaction leading to aggregation and quenching of excited states after photon absorption increases. Because of the number and variety of differently charged groups in these conjugates (both on the pL chain and on the  $c_{e6}$  molecule), it is difficult to predict the effects of intermolecular and intramolecular attraction and repulsion with increasing SRs, and in addition it is likely to be highly pH dependent. Measurements of fluorescence will give some idea of how the tetrapyrrole molecules interact, as it is known that when two planar fluorophores are situated near to each other the absorbed energy can be transferred between them increasing the proportion of non-radiative energy loss. The relationship between the fluorescence and absorption depicted a-c illustrate this point. In all cases (cationic, neutral and anionic) the fluorescence is much higher in NaOH than in PBS presumably because the ionization of the two remaining carboxyl groups on each  $c_{e6}$  moiety increase the steric repulsion between neighboring  $c_{e6}$  molecules on either the same pL chain or neighboring pL chains. For the cationic conjugates in PBS the tendency for the highest SR to have greater fluorescence presumably reflects the higher number of carboxyl groups and the greater likelihood of their being ionized and repelling each other. For the neutral conjugates where the opposite is true, the explanation is less obvious but may involve the absence of positively charged amino groups on the chain influencing the ionization of the  $c_{e6}$  carboxyl groups. In the case of the anionic conjugates the effect of the large number of carboxyl groups on the chain presumably outweighs the effect of the 2 carboxyl groups on the  $c_{e6}$  and thus allows all SRs to behave similarly.

The data from the cell uptake experiments show interesting variations depending on all three variables, cell type, conjugate charge and SR. As we have reported previously [15], a neutral pL- $c_{e6}$ -ac conjugate showed significantly higher uptake by J774 cells compared to OVCAR-5 cells, and the present results extend this selectivity to the lower SRs of cationic conjugate and all SRs of anionic conjugates. Macrophages are well known to be likely to take up macromolecules by various phagocytic and endocytic processes and the tendency of these conjugates to aggregate at neutral pH values may only accentuate this tendency. In a previous publication [13] we showed that the order of cell uptake (by two cell lines) of a single SR set of pL- $c_{e6}$  conjugates with cationic, neutral and anionic charges was cationic > anionic > neutral, while in the present study the order of the last two is reversed with cationic > neutral > anionic. It should be noted that the SR in the present study was higher than 16 (being about 20) and the order of uptake for SR 16 and J774 cells in the present study was cationic > anionic > neutral, so it is possible that higher SRs encourage the uptake of anionic conjugate at the expense of neutral conjugate. The observed increase in uptake with increasing SR (up to 12 for cationic and neutral conjugates, and up to 16 for anionic conjugates) therefore suggests that the binding to the cells is mediated more by the  $c_{e6}$  than the pL chain (of whatever charge). Since the different SR conjugates were delivered to the cells at equal concentrations of  $c_{e6}$ , this means that the lower SRs had significantly higher concentrations of pL chains delivered to the cells than the higher SRs. If the affinity of the conjugates of varying SRs for the cells was equal then one might expect equal uptakes [25], i.e., the SR16 was present in one quarter of the concentration compared to the SR4 conjugate, but each molecule taken up by the cell delivered four times the amount of  $c_{e6}$  herefore the affinity of the conjugate for the cell must increase with increasing SR until a maximum is reached in the case of the cationic and neutral conjugates around SR12.

The confocal micrographs show variations in both intensity and subcellular localization of the red  $c_{e6}$  fluorescence. It is clear that the level of fluorescence in the confocal images does not necessarily correlate with the level of cell uptake (compare neutral SR 16 in both cell lines that has the largest uptake and lowest fluorescence, while SR16 anionic conjugate has highest uptake and highest fluorescence).

The phototoxicity experiments showed that the neutral conjugates were much more phototoxic than either cationic or anionic conjugates in both cell lines especially for the SR 3. This finding is in agreement with our previous reports [13,15] studying acetylated pL- $c_{e6}$  conjugates with a single SR. We showed that a neutral acetylated pL- $c_{e6}$  conjugate was more than 200 times as phototoxic for each dye molecule taken up by A431 tumor cells and endothelial cells compared to cationic and anionic conjugates [13]. The cationic conjugates showed higher phototoxicity towards J774 macrophages compared to OVCAR cells, which correlates with the higher uptake by the J774 cell line. The anionic conjugates showed a tendency to be more phototoxic towards the OVCAR cancer cells compared to the J774 cells. The explanation for these findings probably lies in the different cellular localizations in the 2 cell lines. Macrophages are more likely to accumulate these conjugates (esp gates) in lysosomes due to their macromolecular nature and phagocytic nature of the cells, and many reports suggest that PS are proportionately less phototoxic in lysosomes [26] than in intracellular membrane locations including mitochondria [27,28]. The relative lack of phototoxicity of the neutral SR16 conjugate towards both cell lines despite its high uptake must presumably reflect loss of photoactivity due to quenching and aggregation as evidenced by the relative loss of fluorescence seen in solution Fig. 2a, and low levels of red fluorescence in the confocal micrographs. Conversely the SR 16 of the anionic conjugates gives high uptake, bright fluorescence in the confocal micrographs and shows the highest phototoxicity. It may be possible to use the maintenance of fluorescence levels in cells with rising levels of uptake, as a predictor of subsequent phototoxic efficiency for particular PS or conjugates.

## 6. Conclusions

The chief conclusions from the study can be summarized as follows.

- a) In PBS the fluorescence of all the conjugates is less than in NaOH, while in the cationic series the fluorescence is proportional to SR, in the neutral series the fluorescence is inversely proportional to SR, and in the anionic series there is no difference.
- b) The cellular uptake is higher by J774 macrophages compared to OVCAR-5 cancer cells for all conjugates, the cationic and anionic series show a maximum uptake at a SR of 12, while the neutral series have the highest uptake at a SR of 16.
- c) The cationic and neutral series show proportionately less fluorescence in confocal micrographs at higher SRs where they appear to be aggregated, while the anionic series show much higher fluorescence at high SRs.
- d) The neutral series shows the highest phototoxicity, the cationic series preferably kills J774 cells and the anionic series preferably kills OVCAR-5 cells. For the cationic and neutral series the SR 12 is the most phototoxic, while for the anionic series it is the SR 16.

## Acknowledgments.

This work was funded by the National Institutes of Health (R01 CA/AI838801-A2) and Department of Defense (N00014-94-1-0927). We thank Prof. Tayyaba Hasan for encouragement and support and Dr Paal Selbo for a critical reading of the manuscript.

## References

- [1] M.R. Hamblin and E.L. Newman, On the mechanism of the tumour-localising effect in photodynamic therapy, *Journal of Photochemistry and Photobiology* **B(23)** (1994), 3–8.
- [2] B.W. Henderson and D.A. Bellnier, Tissue localization of photosensitizers and the mechanism of photodynamic tissue destruction, *Ciba Foundation Symposium* **146** (1989), 112–125.
- [3] T. Hasan, Photosensitizer delivery mediated by macromolecular carrier systems, in: *Photodynamic Therapy, Basic Principles and Clinical Applications*, B. Henderson and T. Dougherty, eds, Marcel Dekker, 1992, pp. 187–200.
- [4] A. Bernstein, E. Hurwitz, R. Maron, R. Arnon, M. Sela and M. Wilchek, Higher antitumor efficacy of daunomycin when linked to dextran, in vivo and in vitro studies, *Journal of the National Cancer Institute* **60** (1978), 379–384.
- [5] F. Zunino, G. Savi, F. Giuliani, R. Gambetta, R. Supino, S. Tinelli and G. Pezzoni, Comparison of antitumor effects of daunorubicin covalently linked to poly-L-amino acid carriers, *European Journal of Cancer and Clinical Oncology* **20** (1984), 421–425.
- [6] L.W. Seymour, R. Duncan, P. Kopeckova and J. Kopecek, Daunomycin and adriamycin N (2 hydroxypropyl) methacrylamide copolymer conjugates; toxicity reduction by improved drug-delivery, *Cancer Treatment Reviews* **14** (1987), 319–327.
- [7] N.L. Krinick, Y. Sun, D. Joyner, J.D. Spikes, R.C. Straight and J. Kopecek, A polymeric drug delivery system for the simultaneous delivery of drugs activatable by enzymes and/or light, *Journal of Biomaterial Science Polymer Edition* **5** (1994), 303–324.
- [8] N. Davis, D. Liu, A.K. Jain, S.Y. Jiang, F. Jiang, A. Richter and J.G. Levy, Modified polyvinyl alcohol-benzoporphyrin derivative conjugates as phototoxic agents, *Photochemistry and Photobiology* **57** (1993), 641–647.
- [9] M.R. Hamblin, J.L. Miller and T. Hasan, Effect of charge on the interaction of site-specific photoimmunoconjugates with human ovarian cancer cells, *Cancer Research* **56** (1996), 5205–5210.
- [10] M.R. Hamblin, M.P. Bamberg, J.L. Miller and T. Hasan, Cationic photoimmunoconjugates between monoclonal antibodies and hematoporphyrin, selective photodestruction of ovarian cancer cells, *Applied Optics* **37** (1998), 7184–7192.
- [11] L.R. Duska, M.R. Hamblin, M.P. Bamberg and T. Hasan, Biodistribution of charged F(ab')<sub>2</sub> photoimmunoconjugates in a xenograft model of ovarian cancer, *British Journal of Cancer* **75** (1997), 837–844.
- [12] M.R. Hamblin, M.D. Governatore, I. Rizvi and T. Hasan, Biodistribution of charged 17.1A photoimmunoconjugates in a murine model of hepatic metastasis of colorectal cancer, *British Journal of Cancer* **83** (2000), 1544–1551.
- [13] N.S. Soukos, M.R. Hamblin and T. Hasan, The effect of charge on cellular uptake and phototoxicity of polylysine chlorin(e<sub>6</sub>) conjugates, *Photochemistry and Photobiology* **65** (1997), 723–729.
- [14] M.R. Hamblin, M. Rajadhyaksha, T. Momma, N.S. Soukos and T. Hasan, In vivo fluorescence imaging of the transport of charged chlorin e<sub>6</sub> conjugates in a rat orthotopic prostate tumour, *British Journal of Cancer* **81** (1999), 261–268.
- [15] M.R. Hamblin, J.L. Miller, I. Rizvi, B. Ortel, E.V. Maytin and T. Hasan, Pegylation of a chlorin(e<sub>6</sub>) polymer conjugate increases tumor targeting of photosensitizer, *Cancer Research* **61** (2001), 7155–7162.
- [16] M.R. Hamblin, D.A. O'Donnell, N. Murthy, K. Rajagopalan, N. Michaud, M.E. Sherwood and T. Hasan, Polycationic photosensitizer conjugates: effects of chain length and Gram classification on the photodynamic inactivation of bacteria, *Journal of Antimicrobial Chemotherapy* **49** (2002), 941–951.
- [17] N.S. Soukos, L.A. Ximenez-Fyvie, M.R. Hamblin, S.S. Socransky and T. Hasan, Targeted antimicrobial photochemotherapy, *Antimicrobial Agents and Chemotherapy* **42** (1998), 2595–2601.
- [18] M.R. Hamblin, D.A. O'Donnell, N. Murthy, C.H. Contag and T. Hasan, Rapid control of wound infections by targeted photodynamic therapy monitored by in vivo bioluminescence imaging, *Photochemistry and Photobiology* **75** (2002), 51–57.
- [19] M.A. Markwell, S.M. Haas, L.L. Bieber and N.E. Tolbert, A modification of the Lowry procedure to simplify protein determination in membrane and lipoprotein samples, *Analytical Biochemistry* **87** (1978), 206–210.
- [20] J.L. Merlin, S. Azzi, D. Lignon, C. Ramacci, N. Zeghari and F. Guillemin, MTT assays allow quick and reliable measurement of the response of human tumour cells to photodynamic therapy, *European Journal of Cancer* **28A** (1992), 1452–1458.
- [21] T.J. Dougherty, C.J. Gomer, B.W. Henderson, G. Jori, D. Kessel, M. Korbek, J. Moan and Q. Peng, Photodynamic therapy, *Journal of the National Cancer Institute* **90** (1998), 889–905.
- [22] M. Korbek and G. Kros, Photofrin accumulation in malignant and host cell populations of various tumours, *British Journal of Cancer* **73** (1996), 506–513.
- [23] M. Korbek, G. Kros, J. Kros and G.J. Dougherty, The role of host lymphoid populations in the response of mouse EMT6 tumor to photodynamic therapy, *Cancer Research* **56** (1996), 5647–5652.
- [24] M. Korbek, Induction of tumor immunity by photodynamic therapy, *Journal of Clinical Laser Medicine and Surgery* **14** (1996), 329–334.
- [25] M.R. Hamblin, J.L. Miller and B. Ortel, Scavenger-receptor targeted photodynamic therapy, *Photochemistry and Photobiology* **72** (2000), 533–540.

- [26] C.W. Lin, J.R. Shulok, S.D. Kirley, C.M. Bachelder, T.J. Flotte, M.E. Sherwood, L. Cincotta and J.W. Foley, Photodynamic destruction of lysosomes mediated by Nile blue photosensitizers, *Photochemistry and Photobiology* **58** (1993), 81–91.
- [27] D. Kessel and Y. Luo, Photodynamic therapy, a mitochondrial inducer of apoptosis, *Cell Death and Differentiation* **6** (1999), 28–35.
- [28] D.J. Granville, C.M. Carthy, H. Jiang, G.C. Shore, B.M. McManus and D.W. Hunt, Rapid cytochrome c release, activation of caspases 3, 6, 7 and 8 followed by Bap31 cleavage in HeLa cells treated with photodynamic therapy, *FEBS Letters* **437** (1998), 5–10.